

LivHeart: A Multi Organ-on-Chip Platform to Study Off-Target Cardiotoxicity of Drugs Upon Liver Metabolism

Erika Ferrari, Roberta Visone, Elisa Monti, Enrica Torretta, Matteo Moretti, Paola Occhetta, and Marco Rasponi*

The drug discovery and development process is still long, costly, and highly risky. The principal attrition factor is undetected toxicity, with hepatic and cardiac toxicities playing a critical role and being the main responsible of safety-related drug withdrawals from the market. Multi Organs-on-Chip (MOoC) represent a disruptive solution to study drug-related effects on several organs simultaneously and to efficiently predict drug toxicity in preclinical trials. Specifically focusing on drug safety, different technological features are applied here to develop versatile MOoC platforms encompassing two culture chambers for generating and controlling the type of communication between a metabolically competent liver model and a functional 3D heart model. The administration of the drug Terfenadine, a cardiotoxic compound liver-metabolized into the non-cardiotoxic Fexofenadine, proved that liver metabolism and a fine control over drug diffusion are fundamental to elicit a physio-pathological cardiac response. From these results, an optimized LivHeart platform is developed to house a liver model and a cardiac construct that can be mechanically trained to achieve a beating microtissue, whose electrophysiology can be directly recorded *in vitro*. The platform is proved able to predict off-target cardiotoxicity of Terfenadine after liver metabolism both in terms of cell viability and functionality.

1. Introduction

Drug discovery and development is a long, costly, and high-risk process that takes about 10 years with an average cost of over \$1.5 billion for each new drug to be approved for clinical use.^[1] One of the reasons resides in the fact that ≈90% of candidate drugs are discarded just in the clinical trial phases.^[1] Unmanageable toxicity represents a major attrition factor, accounting for overall 30% of such failures,^[2] led by hepatic and cardiac adverse effects.^[3] Furthermore, drug-induced cardiac and hepatic adverse effects together account for more than 75% of safety-related withdrawals from the market of FDA-approved drugs.^[4] This indicates that currently used preclinical methods to evaluate drug safety, mostly relying on 2D cell cultures and animal models, are not enough predictive of human-related outcomes.^[5] Recently, building upon microfluidics and microfabrication technologies, great

efforts have been spent to develop advanced human microengineered tissue models better representing human physiology for *in vitro* drug screening and safety applications. In this scenario, Organs-on-Chip (OoC) represent innovative and reliable tools to model essential functions of human organs *in vitro*^[6] and have proved unprecedented advantages over both previously mentioned traditional preclinical systems in terms of clinical translational power.^[7] Different OoC solutions encompassing single organs (i.e. liver or heart) have been proposed to perform drug safety studies.^[8–11] However, only few platforms have been developed, able to combine detection of both target and off-target effects of drugs, efficiently reproducing the *in vivo* drug metabolism processes.^[12–14] Multi Organ-on-Chip (MOoC) represent a disruptive solution to study drug-related effects on several organs simultaneously, holding great promises to efficiently predict drug toxicity in preclinical trials and ultimately to prevent unexpected clinical drug safety issues.^[15] In particular, great interest has arisen on liver-heart models that can mimic and predict off-target cardiac toxicity after liver metabolism of drugs.^[8] In this context, Oleaga et al.,^[16] developed a pumpless gravity-driven MOoC platform composed by five chambers integrating liver and heart modules able to predict the cardiotoxic side-effects of Cyclophosphamide and Terfenadine after liver metabolism. This commercial device was also adopted for pharmacokinetic drug studies^[17] Another example


E. Ferrari, R. Visone, E. Monti, P. Occhetta, M. Rasponi
Department of Electronics, Information and Bioengineering
Politecnico di Milano
20133 Milan, Italy
E-mail: marco.rasponi@polimi.it

R. Visone, P. Occhetta
BiomimX Srl
20157 Milan, Italy

E. Torretta
Laboratory of Proteomics and Separative Sciences
IRCCS Istituto Ortopedico Galeazzi
20157 Milan, Italy

M. Moretti
Cell and Tissue Engineering Lab
IRCCS Istituto Ortopedico Galeazzi
20157 Milan, Italy

M. Moretti
Regenerative Medicine Technologies Lab
Ente Ospedaliero Cantonale (EOC)
6962 Lugano, Switzerland

 The ORCID identification number(s) for the author(s) of this article can be found under <https://doi.org/10.1002/admt.202201435>.

© 2023 The Authors. Advanced Materials Technologies published by Wiley-VCH GmbH. This is an open access article under the terms of the Creative Commons Attribution License, which permits use, distribution and reproduction in any medium, provided the original work is properly cited.

DOI: 10.1002/admt.202201435

is the Ex vivo Console of Human Organoids (ECHO) developed by Skardal et al.^[18] The platform is a perfusion-driven and modular microfluidic system designed to study physiological responses of cardiac organoids to liver-metabolized pharmaceuticals. Liver and heart organoids were also implemented in a dual-chamber polydimethylsiloxane (PDMS) platform recently developed by Yin et al.,^[19] where the effects of liver-metabolized Clomipramine were evaluated. Despite promising, the above-mentioned platforms suffer from common drawbacks: host 2D cultures, require high priming volumes and the compartments are not fluidically separated causing uncontrolled interorgan crosstalk. To overcome these limitations, we implemented different technological features in a MOoC encompassing two culture chambers for generating and controlling the communication between a liver and a cardiac model. The liver compartment is based on the micropatterned coculture (MPCC) functional model in a dual-chamber microfluidic platform, that we previously developed and successfully exploited to study the effects of liver-metabolized anticancer drugs on tumor cells.^[20] The heart compartment is based on the 3D beating heart-on-chip^[21] integrated with a system of electrodes to continuously evaluate the electrical activity of cardiac microtissues.^[22] We first present two simplified microfluidic devices, based on either microgrooved channels or pneumatic valves (namely μ Channels and Valve devices, respectively), which were specifically developed aiming at i) investigating the proper communication mechanism to connect and control the crosstalk between the two organ compartments, ii) optimizing the culture parameters, iii) and preliminary assessing the potential of such liver-heart system in drug safety applications. Subsequently, a comprehensive and optimized MOoC platform, the “LivHeart,” is presented and upon validation by administering Terfenadine, proved to be a promising tool for drug screening and safety applications.

2. Results and Discussion

2.1. μ Channels and Valve Devices Fabrication and Characterization

To develop a heart and liver MOoC device able to avoid undesired cross-talk between the models, two different approaches were pursued, which differ on the mechanism of communication between the two organ compartments.

The μ Channels device is composed by two culture chambers which are compartmentalized through an array of microgrooves (Figure 1A(i)). Microgrooves provide a means to confine the two cellular constructs (i.e., hepatic and cardiac cultures) during seeding and allow their continuous fluidic communication once the cultures are established. In particular, the left chamber is designed to host the MPCC liver model and encompasses a single inlet and a single outlet for cell seeding and medium replenishment (Figure 1A(ii), pink). Conversely, the cardiac chamber (right), includes two channels, separated by a row of trapezoidal posts, for the confinement of a 3D cell laden hydrogel and to host the culture medium, respectively (Figure 1A(ii), blue). This design allows the diffusion of soluble factors between the two compartments while excluding direct

cell–cell interactions and minimizing convective transport. To characterize the device's technical functionality and to determine the pattern of solute diffusion between the two culture chambers, the fluorescent molecule Rhodamine was chosen as model compound for diffusion tests. Indeed, Rhodamine has a molecular weight (MW) of 479 g mol⁻¹^[23] which is similar to the drugs adopted in this study (Terfenadine, $M_w = 471.673$ g mol⁻¹ and Fexofenadine, $M_w = 501.68$ g mol⁻¹) and thus it provides a good representation of their behavior. In particular, Rhodamine was administered in the liver compartment and was monitored for 8 h to examine its propagation toward the heart compartment. As shown in Figure 1A(iii), Rhodamine slowly diffused from the liver to the heart chamber and after 1 h its presence was already appreciated in the entire length of the microgrooves. This timing is compatible with the analytical estimation performed by using the Fick's laws of diffusion, which gave a value of 34 min for Rhodamine to fill the microgrooves. After 8 h, 20% of Rhodamine diffused in the heart chamber, as measured along an imaginary line placed 0.2 mm far from the microgrooves.

The Valves device (Figure 1B(i)) instead is composed by two functional overlaying layers: i) a communication valve system layer (top, dark gray) and ii) a chambers layer (bottom, light gray) where liver (Figure 1B(ii), pink) and heart (Figure 1B(ii), blue) compartments are separated by thin PDMS walls (Figure 1B(ii), transparent). Such configuration defines valves which are normally closed, and may be opened when a negative pressure is applied in dedicated valve channels.^[24] Thanks to the integration of such Valve system layer, species transport is completely absent when the communication valve is closed, and diffusion only occurs once the valves are opened, thus providing the user with full temporal control on the system (Figure 1B(iii)). To evaluate the value of negative pressure required to fully open the valves, the valve layer was first prefilled with a green color dye and subsequently pressure was decreased stepwise. At every step the membrane on top of the valves moved upward, moving away the dye and making the wall recover the transparent color (Figure 1B(iv)). The calibration curve of the communication valve system, obtained by measuring the mean gray intensity over the wall, shows that the valve slowly opened, starting from a negative pressure of -100 mmHg and reaching its maximum aperture at -200 mmHg (when no color dye can be detected anymore). This demonstrated the valve platform ability to specifically control the diffusion of soluble molecules between the liver and the heart compartments by opening/closing the communication valve system. In fact, the valve system allows to confine a compound in one compartment (e.g., in the liver for the hepatic drug metabolism) and release it toward the other one (e.g., in the cardiac compartment) when needed. In this way, the effects of a drug and/or a drug's metabolite on cardiac cells after liver metabolism can be accurately studied. To determine the diffusion profile of compounds, fluorescent Rhodamine was administered in the liver compartment; once the valves were opened, Rhodamine diffusion toward the heart compartment (previously filled with phosphate buffered saline (PBS)) was monitored for 1 h. In contrast to the μ Channels device, in the Valve device the equilibrium between the chambers was reached within 1 min of observation, as measured along a preset line placed 0.2 mm far from the left border of the heart chamber (Figure 1B(v)).

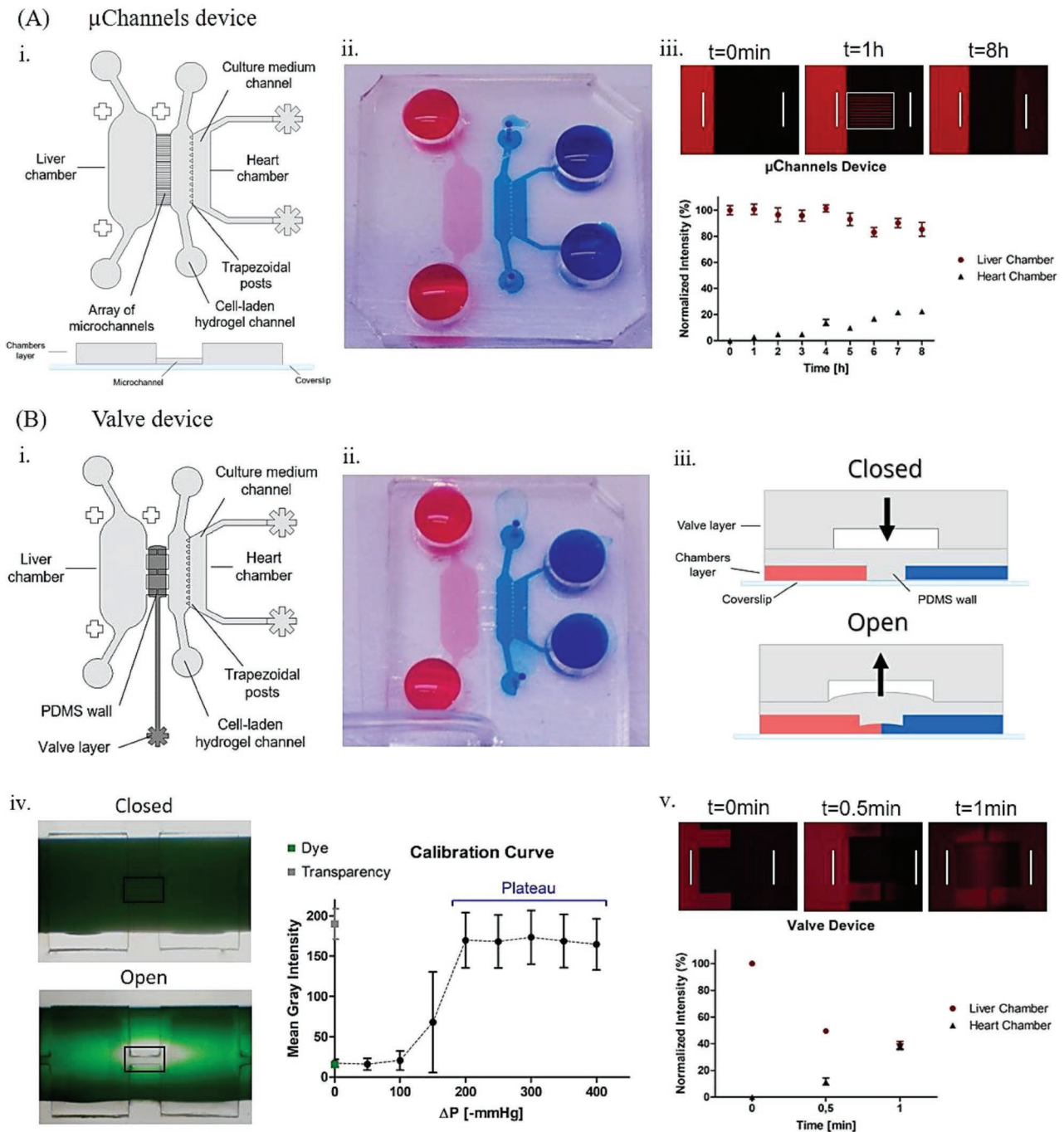


Figure 1. Layout and characterization of the μ Channels and Valve devices. A) (i) Layout of the μ Channels platform. The left chamber is conceived for a 2D hepatic culture and the right chamber for a 3D cardiac culture. The two culture chambers are compartmentalized by an array of microgrooves that provide a means to confine the two cellular constructs during seeding and allow their continuous fluidic communication once the cultures are established. (ii) Picture of the fabricated μ Channels platform. The liver and heart chambers are highlighted in pink and blue, respectively. (iii) Diffusion characterization of the μ Channels platform using Rhodamine injected in the liver chamber. The pattern of solute diffusion was monitored for 8 h and measured along the white lines. B) (i) Layout of the Valve platform composed by a communication valve system layer (dark gray) and a chambers layer (light gray), where the liver and heart chambers are separated by thin PDMS walls. These isolate the culture chambers and can be opened through the application of a negative pressure in the valve layer. (ii) Picture of the fabricated Valve platform. The liver and heart chamber are highlighted in pink and blue, respectively. (iii) Working principle: the application of a negative pressure in the valve layer deflects upward the PDMS walls, enabling the communication between the liver and heart compartments. (iv) Calibration curve of the valve opening pressures, obtained through the calculation of gray intensity values in the selected region of interest (i.e., black squares) during the application of decreasing values of pressure. The deflection of the PDMS walls toward the valve system, which was prefilled with a green-colored dye (closed configuration), moved away the dye and the transparent color was recovered when the maximum suction effect is reached (opened configuration). (v) Diffusion characterization of the Valve platform using Rhodamine injected in the liver chamber. In contrast to the μ Channels device, the equilibrium between the chambers was reached within 1 min, as measured along the white lines.

2.2. Cell Viability and Functionality Assessment

MPCC of HepG2 and NIH-3T3 fibroblasts were successfully generated in the liver compartment^[20] of both μ Channels and Valve platforms, together with the 3D myocardial model composed by cardiomyocytes and cardiac fibroblasts (Figure 2A).^[21] After 1 day from the seeding, the hepatic islands showed the typical circular shape that was maintained till day 7 of culture (Figure 2B(i)). Neonatal rat cardiomyocytes (NRCM) were successfully embedded in fibrin hydrogel and demonstrated to be able to remodel the fibrin matrix and to assume an interconnected morphology after 7 days in culture (Figure 2B(ii)). At the functional level, micropatterned HepG2 of the liver chamber maintained their biological function, as demonstrated by the good albumin production at day 7 of culture evidenced

by the immunofluorescence staining of the secreted molecule (Figure 2C(i)). NRCMs started to spontaneously beat at day 3 of culture and after 7 days in culture (Figure 2C(ii)) expressed a typical cardiomyocytes marker (i.e., troponin I, green) and the marker of gap-junction (i.e., Cx43, pink). Both MPCC and NRCM constructs showed a high viability that was maintained up to 1 week of culture in both devices (Figure 2D). In particular, MPCC construct viability resulted around $90.5\% \pm 2.5\%$ at day 1 and $87\% \pm 3.5\%$ at day 7 in μ Channels device (Figure 2D(i)), and around $91\% \pm 3\%$ at day 1 and $84\% \pm 2\%$ at day 7 in the Valve device (Figure 2D(ii)). In turn, the NRCM construct viability resulted around $93\% \pm 2\%$ at day 1 and $88\% \pm 2.5\%$ at day 7 in μ Channels device (Figure 2D(i)), and around $94\% \pm 1.5\%$ at day 1 and $90\% \pm 2\%$ at day 7 in the Valve device (Figure 2D(ii)). Such viability data are compatible with

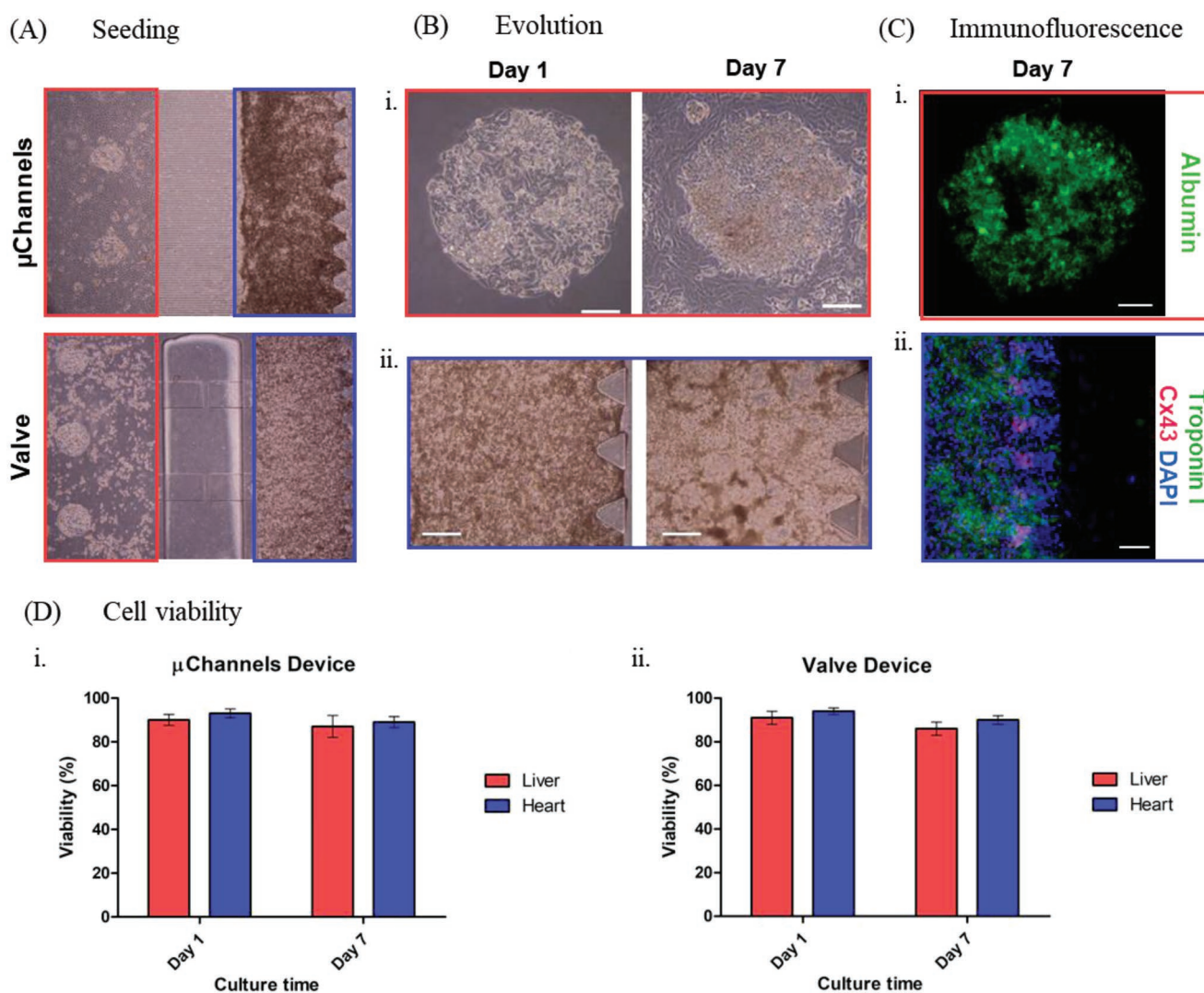


Figure 2. Liver-Heart model where the red rectangle highlights the hepatic model, and the blue rectangle shows the cardiac model. A) The hepato-cardiac coculture generated within the μ Channels and Valve devices after the seeding. B) Evolution of the (i) hepatic islands and (ii) the NRCM embedded in the fibrin matrix at the beginning (day 1) and at the end (day 7) of the culture period. Scale bars of $100\ \mu\text{m}$ for the hepatic model. Scale bars of $250\ \mu\text{m}$ for the cardiac model. C) Immunofluorescence images of (i) albumin (i.e., green) content in the hepatic island, and (ii) Troponin I (i.e., green), Connexin 43 (i.e., Cx43, red), and DAPI (i.e., blue) contents in the cardiac model. Scale bars $100\ \mu\text{m}$. D) Cell viability of the hepato-cardiac coculture at the beginning and at the end of the culture period in the (i) μ Channels and (ii) Valve devices.

previous work on liver^[20] and cardiac^[21,22,25] cultures within microfluidic devices.

2.3. Toxicity of Terfenadine in μ Channels and Valve Devices

Terfenadine (TER) is an antihistaminic compound affecting multiple cardiac ion-channels (i.e., block K⁺ and Ca²⁺ currents) and it is able to cause a prolongation of the heart depolarization-repolarization interval (i.e., QT interval), which may lead to severe cardiotoxic effects.^[26] In the human liver, the enzymes of the cytochrome P450 metabolize and reverse the toxicity of TER transforming it into its noncardiotoxic form, Fexofenadine (FEX). FEX has the same antihistaminic effect of TER but does not show any cardiac side issue.^[27] To reproduce the in vivo complexity of the above-mentioned phenomenon and to screen the effect of pro- and metabolized-drugs, both μ Channels and Valve devices were used. As outlined in the experimental plan (Figure 3A), after 5 days in culture, when both models resulted developed, 10 μ M of Terfenadine was administered into the hepatic compartment to be metabolized by MPCC. In particular, in the μ Channels device the drug administered in the liver compartment starts to immediately diffuse toward the heart compartment, while concurrently being metabolized by the liver, since the culture chambers are in continuous communication. This means that in the heart compartment both parent (TER) and metabolized (FEX) compounds act simultaneously (TER + FEX condition). Conversely, in the Valve device, TER was first allowed to be metabolized in the hepatic

chamber. After 16 h the communication valve system was actuated, allowing the metabolized drug (TER \rightarrow FEX condition) to diffuse in the heart chamber (i.e., 10 h as calculated through Fick's law). As shown in Figure 3B, NRCMs subjected to pure terfenadine (TER) exhibited a low viability as evidenced by the high number of dead cells stained with ethidium (red). The viability quantification showed values of $67\% \pm 4.4\%$, which results in a reduction of viability of about 18% compared to the cells exposed to dimethyl sulfoxide (DMSO), used as negative control. The Terfenadine administered to the hepatic chamber in the μ Channels device (TER + FEX) conversely slightly reduced NRCMs viability (i.e., $78.25\% \pm 7.14\%$); while the same drug administered to hepatocytes in the Valve device (TER \rightarrow FEX) did not affect cardiac viability ($93\% \pm 5.57\%$) as compared to the DMSO control ($84.91\% \pm 10.24\%$). This result confirmed that liver MPCC effectively metabolize TER and transform it into nontoxic FEX. Notably, in the μ Channel platform the viability of cardiac cells exposed to a mixture of TER and FEX (TER + FEX) resulted halfway between TER \rightarrow FEX and pure TER conditions, showing that the liver MPCC were not able to fully metabolize TER into FEX before TER diffuses into the heart compartment and exerts its toxic effect. Conversely, the results obtained with the Valve device highlighted that the liver MPCC were able to fully metabolize the toxic TER and transform it into nontoxic FEX before the molecule diffuses into the cardiac compartment through the opening of the communication valve system. This last condition better recapitulates the physiological condition where the drug is metabolized by the liver before circulating into other organs.^[28,29]

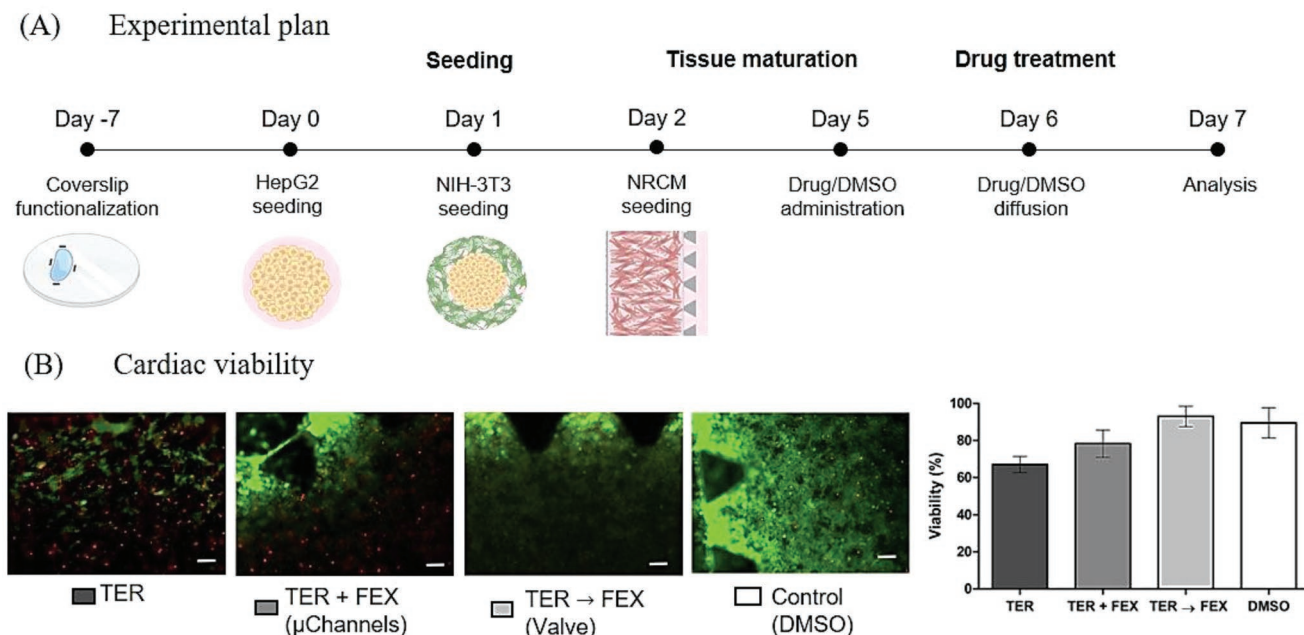


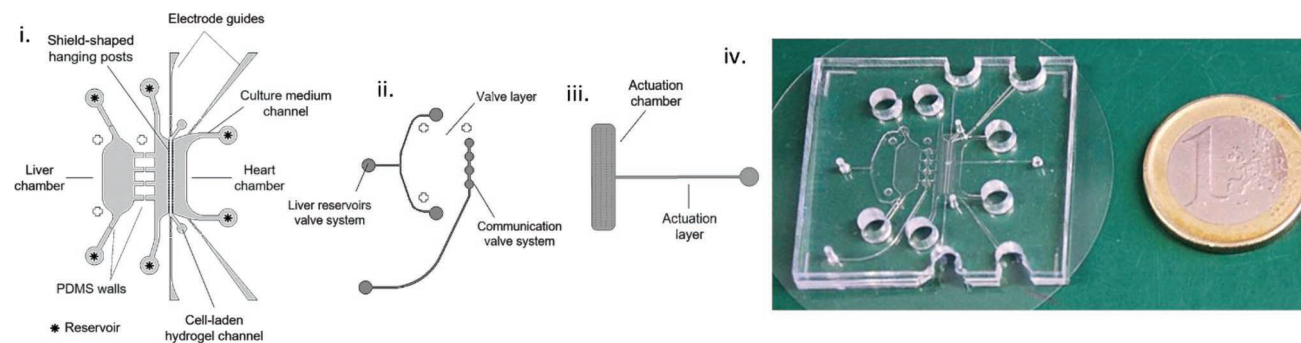
Figure 3. Drug Screening of Terfenadine in the μ Channels and Valve devices. A) Experimental plan. The two microtissues were independently generated and cocultured for 5 days before proceeding with the administration of the drug in the liver compartment. In the μ Channels device, the drug administered started to immediately diffuse toward the heart chamber while concurrently being metabolized by the hepatic model. In the Valve device, the drug was allowed to fully metabolize in the liver chamber for at least 16 h before opening (day 6) the communication valve and letting the metabolized drug (i.e., fexofenadine) diffuse. The effects on cardiac viability of the pro- (TER) and metabolized- (FEX) drugs were investigated through a Live/Dead assay, performed on day 7. B) Cardiac viability after the exposure of NRCMs to Terfenadine (TER, no liver metabolism) and to liver-metabolized Terfenadine in the μ Channels (TER + FEX) and in the Valve (TER \rightarrow FEX) devices.

2.4. LivHeart Concept and Technical Characterization

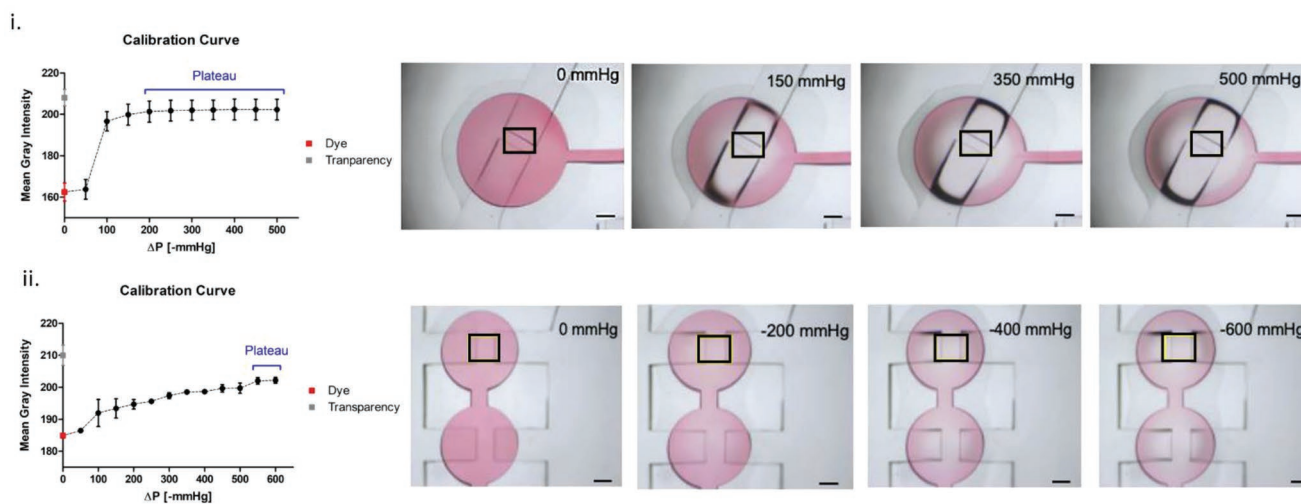
After having confirmed the technical feasibility of the biological models and attested the superior performance of the Valve device in controlling the hepatic metabolism of drugs, a platform specifically designed to improve heart functionality and

to directly monitor the electrophysiological parameters of the heart was developed (i.e., LivHeart). The LivHeart (Figure 4A) is composed by three functional layers: i) a chambers layer (bottom) for liver and heart cultures (Figure 4A(i)), ii) a valve layer (middle) housing the liver-reservoir valve system and the communication valve system (Figure 4A(ii)), and iii) an

(A) LivHeart Layout



(B) Valve systems characterization



(C) Strain characterization

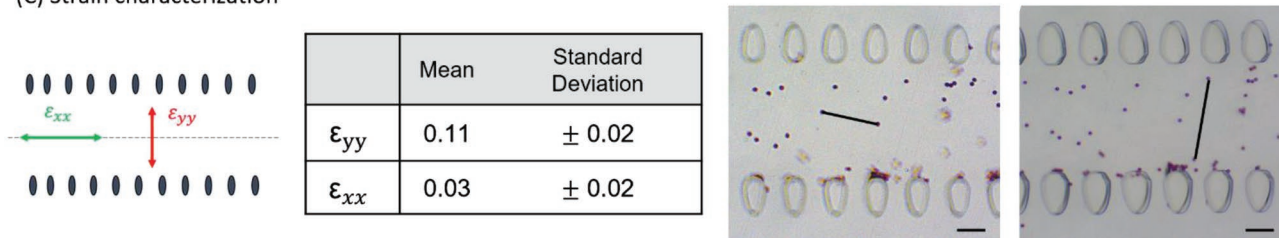


Figure 4. Layout and characterization of the LivHeart device. A) The LivHeart is composed by (i) a chambers layer for the liver and heart cultures, (ii) a valve layer comprising two valve systems (liver-reservoirs and communication valve systems) and (iii) an actuation layer which provides mechanical stimulus to the 3D cardiac microtissue. In the chambers layer, the 3D cardiac culture is confined between two parallel rows of shield-shaped hanging posts and a pair of PDMS walls is placed between the two compartment and between the liver chamber and the corresponding reservoirs. Guides for electrode's insertion needed for the cardiac signal monitoring are included in the design of the heart chamber. (iv) Picture of the fabricated LivHeart device, where the 2 and 4 reservoirs of liver and heart compartment, respectively, are visible as holes in the chip. B) Calibration curves of (i) liver-reservoirs and (ii) communication valve systems opening pressures obtained through the measurement of gray intensity values in the selected regions of interest (i.e., black squares) during the application of decreasing values of pressures. Scale bars are 250 μm . C) Transversal (ϵ_{yy}) and longitudinal (ϵ_{xx}) strains characterization in the mechanically actuated devices, obtained by measuring the distance between couples of beads (i.e., black lines) at rest and during the application of increasing values of pressures. Scale bars are 100 μm .

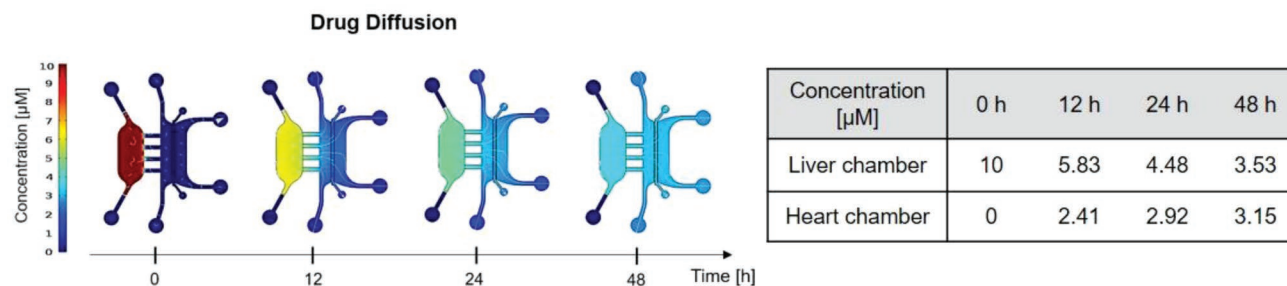
actuation layer (top) (Figure 4A(iii)). The PDMS device is thus obtained by assembling all the PDMS layers and by closing the camber layer at the bottom against a glass coverslip (Figure 4A(iv)). Likewise, in the Valve device, the chambers layer contained thin PDMS walls that in this specific configuration were not only applied to separate liver and heart compartments (communication walls), but also to isolate liver chamber from its medium reservoirs (reservoir walls) (Figure 4A(i)). In the heart compartment, two rows of shield-shaped hanging posts were designed to confine the 3D cardiac microtissue in the central portion of the chamber, flanked by two cell medium channels. In addition, four electrode guides were added in the design to position electrical probes exploited to monitor the cardiac electric signals.^[22] The valve layer (Figure 4A(ii)) is placed on top of the PDMS walls and comprised two independent valve systems: the liver-reservoir valve system aligned on top of the reservoir walls and the communication valve system on top of the communication walls of the chambers layer. Calibration curves for the two independent valve systems showed that the liver-reservoir valve system is fully open at -200 mmHg (Figure 4B(i)), whereas the communication valve system reaches the maximum aperture at -550 mmHg (Figure 4B(ii)). This double (i.e., reservoirs and communication) valve system of the LivHeart platform was designed for two reasons: i) to fully control the better concentration of metabolized drugs in the liver, avoiding any diffusion of molecules to/from the

reservoirs and ii) to control diffusion between the liver and the heart compartments, avoiding convection due to possible hydrostatic pressure unbalances among the 6 reservoirs. The actuation layer is designed to provide a mechanical stimulus to the 3D cardiac microtissue hosted in the cardiac compartment so that the microtissue's functionality is improved, as demonstrated in previous works.^[9,21,30] The mechanical stimulation is achieved by pressurizing the actuation compartment, so to control the movement of the hanging posts bordering the construct toward the coverslip at the bottom. The gap underneath the posts ($50 \mu\text{m}$) indeed is dimensioned so that the microtissue is stretched at physiological values (i.e., 10–15% of strain^[21]) once the posts touch the coverslip (i.e., 500 mmHg). As confirmed by monitoring the movement of polystyrene beads embedded in a fibrin gel (Figure 4C), the strain obtained within the cardiac chamber at 500 mmHg pressure resulted within the physiological range in the transversal direction (ϵ_{yy} value is 0.11 ± 0.02), while being negligible (ϵ_{xx} is 0.03 ± 0.02) in the perpendicular direction.

2.5. Modeling Terfenadine Diffusion within the LivHeart

To analyze the working principle of the LivHeart platform and to determine the diffusion profile of Terfenadine from the hepatic to the heart chamber, finite element models (FEM) were used. Figure 5A shows 2D color maps of Terfenadine

(A) Numerical diffusion simulation



(B) Diffusion characterization

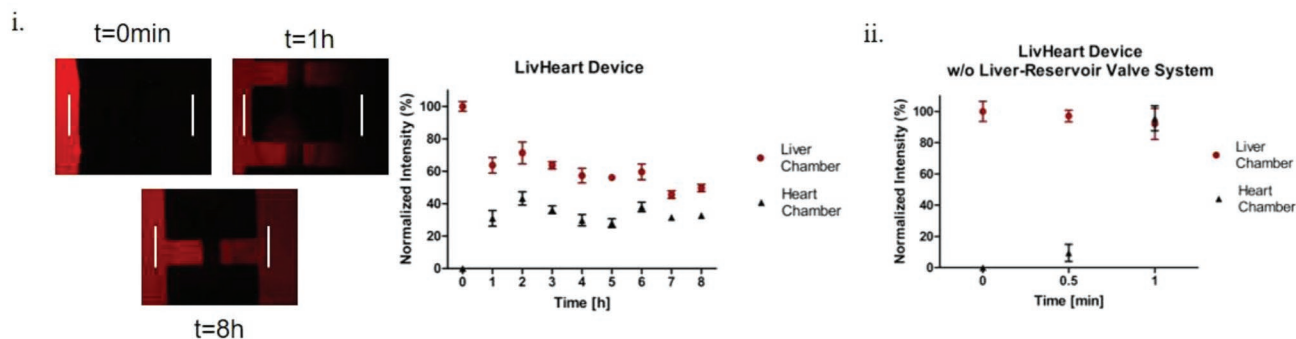


Figure 5. Modeling Terfenadine diffusion within the LivHeart device. A) Numerical diffusion simulation built with COMSOL Multiphysics showing the diffusion profile of a molecule after 0, 12, 24, and 48 h from its administration in the liver compartment. B) Diffusion characterization using Rhodamine injected in the liver chamber. (i) The diffusion of the solute in the liver and heart chambers monitored for 8 h (measured along the white lines) while the liver-reservoir valve system was closed, and the communication valve system was open to let the solute diffuse. (ii) The diffusion of the solute in the liver and heart chambers monitored in the LivHeart without the liver-reservoir valve system.

diffusion between the two compartments at 0, 12, 24, and 48 h upon communication valves aperture and liver-reservoir valves closure. Given an initial drug concentration of $10\ \mu\text{M}$ administered in the liver chamber, at 48 h the drug concentration reaches the plateau value of about $3.15\ \mu\text{M}$ in the cardiac compartment (area between the two hanging posts rows) and $3.53\ \mu\text{M}$ in the hepatic compartment. Indeed, heart compartments' inlets/outlets and reservoirs are not isolated, contributing to the further dilution of the diffusing molecule (i.e., about the 33% of the compound is distributed there), that reached a concentration between the tissues of about the 67% of its initial value. Concentration values at 24 and at 48 h in the cardiac channel are quite similar (i.e., 2.92 vs $3.15\ \mu\text{M}$, respectively), meaning that 24 h may be sufficient for the drug to diffuse and start its activity on the cardiac microtissues. The numerical results found supports from the experimental analysis, obtained by administering Rhodamine in the liver compartment while monitoring its diffusion toward the heart compartments for 8 h (Figure 5B(i)). As expected, Rhodamine could diffuse from the liver to the heart (prefilled with PBS) chamber only after communication valve system aperture. Moreover, the diffusion of fluorescein started to be appreciated in the heart chamber (0.2 mm far from the left border of the heart chamber) after a few minutes from Rhodamine addition, which is compatible with the analytical estimates (2 min by solving Fick's laws of diffusion). In addition, due to the liver-reservoir valve system, convection is completely eliminated, and pure diffusion is thus achieved between compartments. This was further demonstrated by exploiting an ad hoc-designed LivHeart platform without the liver-reservoir valve system, where the connection between the two culture chambers is controlled by the communication valve system only. This configuration led to a diffusive behavior (Figure 5B(ii)) similar to the Valve device, as the equilibrium of fluorescein between the chambers was reached more rapidly (within 1 min of observation).

2.6. Toxicity of Terfenadine in LivHeart Device

MPCC of HepG2 and fibroblast were successfully patterned within the liver chamber of the LivHeart, and NRCM-laden fibrin gel was effectively injected in the heart compartment of the platform. The independent tissue development was also obtained with cardiac microtissue starting to spontaneously beat at day 3 of culture, as expected (Supporting Information Video). For the drug screening, according to the experimental plan outlined in Figure 6A, $10\ \mu\text{M}$ of Terfenadine was administered into the hepatic compartment of the LivHeart device at day 5 of culture, to allow its metabolism by MPCC. TER was allowed to metabolize in the hepatic chamber for 16 h and eventually the communication valve system was opened so that liver-metabolized TER (TER \rightarrow FEX condition) could diffuse in the heart chamber. The effective metabolism of Terfenadine was confirmed by measuring in four samples the percentage of Fexofenadine after 16 h of incubation (Figure 6B, peaks at 2 min), which resulted to account in mean for about the 90% of the total drug present (the 10% represent a Terfenadine residual, Figure 6B, peaks at 2.48 min). The effects on cardiac viability

and electrical functionality of TER \rightarrow FEX were compared to vehicle control (DMSO), Terfenadine condition without liver metabolism (TER) and Fexofenadine condition (FEX) (mass spectrometry measurements confirming the presence of compounds in the media are provided in Supporting Information Figure). In particular, Live/Dead assay and analysis of the variation in the cardiac electrical signals were performed on day 7 of culture. MPCC viability (Figure 6C(i)) was not affected from the incubation and metabolism of Terfenadine ($88.8\% \pm 6.9\%$), maintaining similar values compared to the control ($84.6\% \pm 5.3\%$). Conversely as highlighted in Figure 6C(ii), NRCMs viability was affected by the presence of Terfenadine without liver metabolism (TER, -11.76% viability compared to the control), whereas it was not impaired by the incubation of pure Fexofenadine (FEX, $+5.1\%$ viability compared to the control), or Fexofenadine derived from MPCC-mediated metabolism (TER \rightarrow FEX, -0.14% viability compared to the control). These results are consistent with data from literature^[16] where cardiac cell viability was demonstrated to be severely affected by Terfenadine, decreasing of about 20% and 45% for concentrations of 5 and $10\ \mu\text{M}$, respectively. The slightly less severe Terfenadine-related reduction in cell viability found in the LivHeart may be due to the lower concentration of Terfenadine in the cardiac channel at the time of analysis (i.e., $2.92\ \mu\text{M}$, according to the numerical simulation, Figure 5A), with respect to the concentration shown to be severely harmful for cardiomyocytes.

Concerning the electrical signals acquisition, in all conditions the probes could be correctly positioned (Figure 6D(i)) and the typical field potential signal characterized by the depolarization spike and by the repolarization wave (Figure 6D(ii)) could be acquired to assess the beating period (BP) and field potential duration (FPD) of the cardiac microtissues. The analyses demonstrated that the spontaneous beating frequency decreased in all conditions when compared to the control (DMSO, 2.29 ± 2.12 Hz) (Figure 6D(iii)). In detail, the spontaneous beating frequency of the microtissues upon incubation with Terfenadine (TER) and Fexofenadine (FEX) were similar (0.69 ± 0.56 vs 0.52 ± 0.54 Hz, respectively), whereas the frequency after the incubation with metabolized Terfenadine (TER \rightarrow FEX) was 1.40 ± 1.83 Hz. Thus, compared to the control, the spontaneous beating frequency decreased of about 70%, 40%, and 77% in the TER, TER \rightarrow FEX, and FEX conditions, respectively. The decrease of spontaneous beating frequencies of TER and TER \rightarrow FEX conditions are consistent with the results obtained by Oleaga et al.,^[16] even if the cell source is different (rat CMs here vs hiPSC-CMs). This decrease resulted more accentuated in our platform (-70% vs -42.7% , TER condition) and it may depend on the adopted cell sources, since the heart rate of rats is higher than the human one ($330\text{--}480$ ^[31] vs $60\text{--}100$ bpm, respectively). The lower decrease in the beating frequency evidenced in the TER \rightarrow FEX respect to DMSO, when compared to TER, may be explained by the hepatocyte's metabolism. The metabolically active cells may indeed release factors which positively conditioned the beating, confirming previously reported data evidencing that the presence of hepatocytes slightly increases the beating frequency of cardiac cells.^[16] Another possible explanation is related to the different cell culture conditions (3D in the LivHeart vs 2D in the platform of Oleaga and colleagues). Indeed, spontaneous beating frequency of

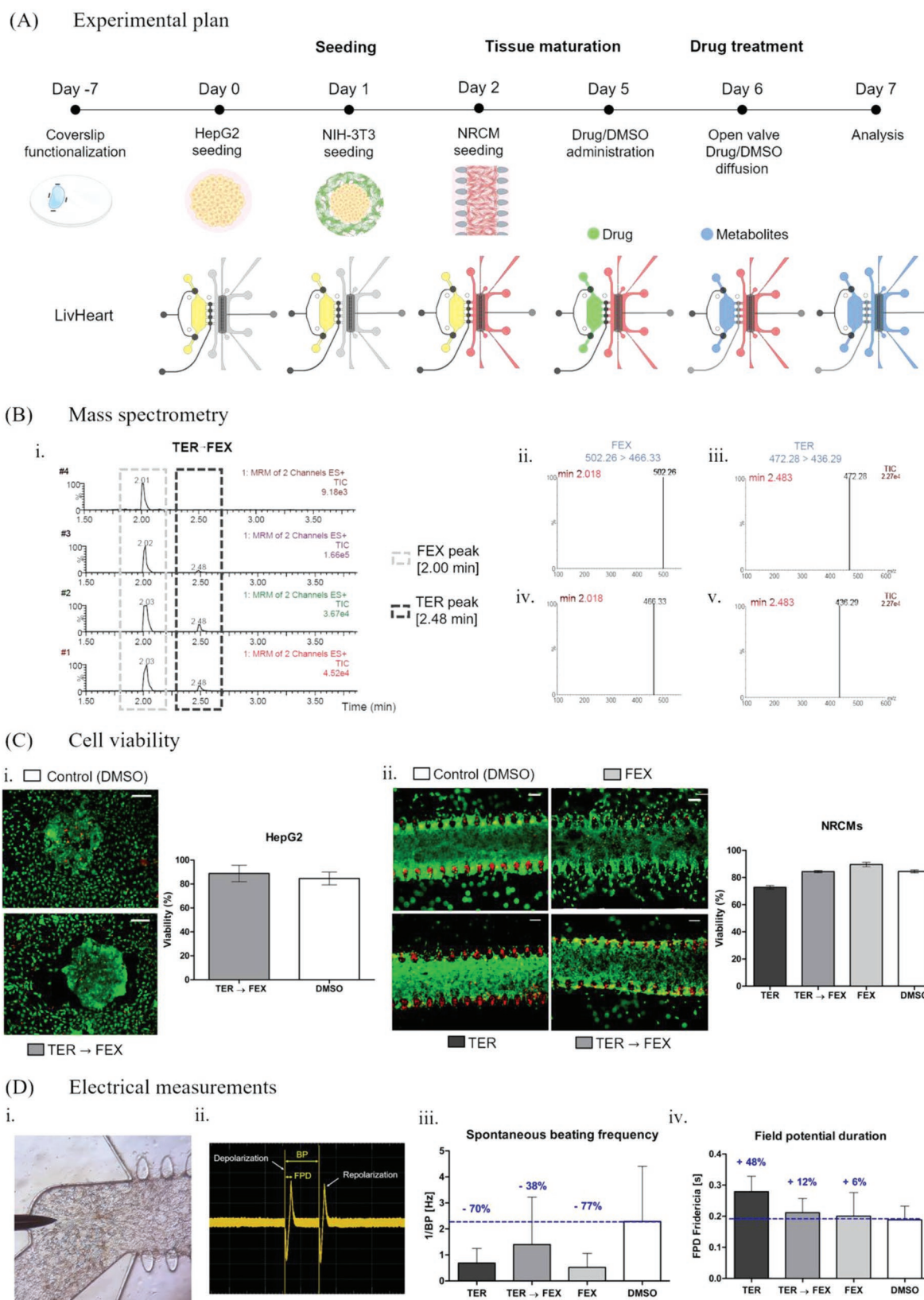


Figure 6. Drug screening with Terfenadine in the LivHeart device. A) Experimental plan. The hepatic and the cardiac models were cultured independently for 5 and 3 days, respectively, before proceeding with the administration of the drug in the liver chamber. The drug was allowed to fully metabolize for at least 16 h and the communication valve system was opened on day 6 so that the liver-metabolized drug could diffuse in the heart

hiPSC-CMs differed between 2D multiwell-like culture condition^[16] and 3D mechanically stimulated heart models^[22] (1 ± 0.05 Hz vs 0.59 ± 0.45 Hz, respectively). The FPD increased only in the TER compared to the control (0.28 ± 0.05 vs 0.19 ± 0.04 s). For what concerns FEX and TER \rightarrow FEX conditions, the FPD values were similar to the control (0.2 ± 0.08 vs 0.21 ± 0.05 s) (Figure 6D(iv)). Thus, the FPD increased of about 48%, 12%, and 6%, compared to the control, after the incubation of Terfenadine without liver metabolism, Terfenadine with liver metabolism and Fexofenadine, respectively. These results are consistent with the potassium channel blockage activity of Terfenadine.^[16] In particular, the FPD prolongation is less accentuated in our platform compared to Oleaga's MOoC (48% vs $117 \pm 39\%$, respectively), probably due to interspecies differences in the FPD interval duration between murine and human cells (200 vs 385 ms)^[32] or due to the different culture conditions (3D vs 2D). Overall, these results indicate that the LivHeart platform is able to fully metabolize toxic Terfenadine and convert it into nontoxic Fexofenadine before the pure diffusive communication with the cardiac compartment is enabled.

3. Conclusions

We successfully developed a versatile MOoC platform to investigate the effects of liver-metabolized drugs on cardiac cells functionality. The use of different platforms (i.e., μ Channels and Valve devices) allows the integration of a metabolically competent liver model (MPCC of HepG2 cells and NIH-3T3 murine fibroblasts) with a 3D heart model (NRCM embedded in a fibrin gel) cultured in two different compartments of the device, and to tailor the type of communication (i.e., continuous and on/off for μ Channels and Valve platforms, respectively) between the two organ models to better understand the diffusion behavior and related efficiency of metabolized drugs. The μ Channels and Valve devices were subjected to the administration of the drug Terfenadine, a cardiotoxic compound metabolized by the liver into Fexofenadine, a noncardiotoxic molecule. Our results proved that the presence of a metabolically competent liver and a controlled drug diffusion are fundamental to mimic in vitro drug biotransformation and to elicit a physiopathological cardiac response. From these preliminary results, a de novo design of a MOoC (LivHeart platform) was conceived, manufactured and tested for drug metabolism and diffusion. In particular, within the LivHeart device, the cardiac construct could be mechanically trained to achieve a physiologically beating microtissue, whose electrical activity could be continuously evaluated. Our results proved the ability of the LivHeart platform to predict off-target cardiotoxicity of Terfenadine after

liver metabolism both by monitoring drug-induced modifications in cell viability and functionality, in a more physiologic way compared to available single-organ microfluidic platforms. To further improve the similarity with the human counterpart, more relevant liver and cardiac cell types (e.g., cardiac and hepatic cells derived from hiPSC) need to eventually be incorporated in our models. The cell lines and primary murine cells used in this work, indeed although being relevant enough to demonstrate the working principle of our platforms, are respectively known to have lower functionality and to suffer from inter-species differences, compared to primary human cells. The LivHeart platform is a further example of how MOoC may represent a disruptive solution to study drug-related effects on off-target organs after liver metabolism, to ultimately improve drug safety testing in the preclinical phases during drug development.

4. Experimental Section

Microdevices Design and Fabrication: To investigate if the presence of a metabolically competent liver could mimic the in vivo side effects of metabolized compounds on the heart, three microfluidic devices were conceived and fabricated: μ Channels, Valve, and LivHeart. Device layouts are characterized by two culture chambers to host the hepatic and the cardiac models. To simulate the complex liver-heart crosstalk, two ways to connect culture chambers were exploited. In the μ Channels device, microgrooves were designed to connect the two culture chambers, whereas in the Valve and LivHeart devices a system of normally closed microfluidic valves was designed between the two compartments. Layouts of the microfluidic devices were generated through specific computer-aided design (CAD) software (AutoCAD, Autodesk Inc., USA). Silicon master molds were fabricated in a cleanroom environment (Polifab, Politecnico di Milano) through SU8 photolithography (MicroChem, USA). After UV (mask aligner, Karl Süss MA6/BA8) or laser light (maskless aligner, Heidelberg MLA100, Heidelberg Instruments) exposure, wafers with features in relief were cured and developed according to the manufacturer's specification.

The microstructured silicon master molds were used for the soft-lithographic process. First, the master molds were subjected to a silanization treatment. Briefly, the mold surface is exposed to tri-methylchloro-silane (Sigma-Aldrich) for 30 min at room temperature, in order to prevent the PDMS from sticking to the wafer and help its removal. PDMS layers (Sylgard 184, Dow Corning; mixing ratio of 10:1 elastomer base:curing agent) were thus fabricated through replica-molding of the master molds. After curing (65 °C for 3 h), PDMS layers were peeled off the mold and assembled by air plasma (Harrick Plasma Inc). In particular, the μ Channels device is directly bonded on a coverslip. In the Valve device, the valve layer is first aligned on top of the chambers layer (still on the silicon master mold) before detaching the two layers (i.e., valve and chambers ones) and finally bonding them to the coverslip. In the LivHeart device, the actuation layer is aligned on top of the valve layer (still on the silicon master mold) and this assembly is detached and aligned on top of the chambers layer before the whole

chamber. The effects on cardiac viability and electrical functionality were analyzed after 24 h of drug incubation in the heart chamber. B) i) MRM chromatograms of TER \rightarrow FEX condition in four independent samples. Fexofenadine metabolized from the hepatic islands after 16 h of Terfenadine incubation was detected at 2 min, whereas residual Terfenadine was detected at 2.48 min; ii) and iii) Representative MRM parent ions of FEX and TER, at 502.26 and 472.28 m/z , respectively; iv) and v) Representative MRM daughter ions of FEX and TER, at 466.33 and 436.29 m/z , respectively. C) Cell viability of (i) hepatic and (ii) cardiac models were monitored through Live/Dead assay. DMSO, vehicle control; TER, Terfenadine; FEX, Fexofenadine; TER \rightarrow FEX, liver-metabolized Terfenadine. Scale bars of 250 μ m (i) and of 100 μ m (ii). D) (i) The electrical activity of the cardiac microtissue was monitored through the insertion of electrodes at the end of the construct. (ii) From the recorded signals, the beating period (BP) interval and the field potential duration (FPD) were measured. (iii) Spontaneous beating frequency value was derived from the mean value of BP intervals and (iv) FPD mean values were corrected with Fridericia correction. In blue, mean values of conditions compared with the mean values of controls.

assembly is eventually bonded on a coverslip. A 4 and 1 mm diameter biopsy punchers were used to punch inlet/outlet of the liver and heart chambers, respectively, and a 1.5 mm diameter biopsy puncher was used to punch valve systems and actuation access ports. Additionally, 5 mm diameter biopsy puncher was adopted to open the access to the guides for electrodes insertion. Figures 1A(ii), B(ii), and 4A(iv) show pictures of the fabricated microfluidic platforms. In the following paragraphs details on the design and fabrication of each platform are presented.

Microdevices Design and Fabrication— μ Channels Device: The μ Channels device was conceived to connect the liver and heart models by an array of 170 microgrooves (1 mm wide, 3 μ m long, and 5 μ m high), designed to both compartmentalize and maintain the communication between the two culture chambers. In detail, the liver chamber was designed as previously described,^[20] with a single inlet and a single outlet for cell seeding and medium replenish. The heart chamber (3 \times 6 \times 0.18 mm) features an inlet and an outlet for cell laden hydrogel injection and one inlet and one outlet for medium replenishment. Cell laden hydrogel and medium channels are separated by a row of trapezoidal posts (channel hosting the 3D cardiac microtissues is 200 μ m wide) needed for hydrogel confinement (Figure 1A(i)). The fabrication of the chambers layer was performed by UV photolithography through a mask aligner machine. Briefly, first flood exposure was first adopted to increase adherence of SU8 features to the silicon wafer, and then the pattern of each layer was transferred on SU8 photoresists, previously spin-coated on 4 in. silicon wafers. Features height was set as follows: 180 μ m for the chambers layer and 5 μ m for the microgrooves. Specifically, to obtain 180 and 5 μ m photoresist layers, the spinning velocity used were 1650 and 4000 rpm for SU8-2100 and SU8-2005, respectively. The microgrooves were fabricated by direct laser writing.

Microdevices Design and Fabrication—Valve Device: The Valve device was conceived to connect the liver and heart models by means of a valve system. The working principle of the platform relies on the use of on/off valves, allowing for the communication or isolation of the two compartments whose design is the same as the μ Channels device. To implement the valve mechanism into the platform, the device featured two different layers: i) the chambers layer (i.e., bottom layer, 180 μ m high) which contains two chambers connected by three dead-end channels where PDMS walls (100 μ m thick and 390 μ m wide) will be generated to isolate the two compartments; ii) the valve layer (i.e., top layer, 180 μ m high) which contains the communication valve system to operate the device. A single rectangular feature (1.2 mm wide and 3.5 mm long) was designed to lift at the same time all the PDMS walls separating the two culture chambers (Figure 1B(i)). The fabrication of the device was performed by UV photolithography through a mask aligner machine. Briefly, flood exposure was first adopted to increase adherence of SU-8 features to the silicon wafer, and then the pattern of each layer was transferred on SU8-2100 photoresist, previously spin-coated on 4 in. silicon wafers. To obtain 180 μ m SU8-2100 photoresist layer, the spinning velocity used was 1650 rpm.

Microdevices Design and Fabrication—LivHeart Device: The LivHeart platform concept reflects the characteristics of the Valve device, in which two culture chambers (i.e., liver, heart) normally isolated by PDMS walls can be connected by means of a communication valve system. Additionally, key elements of the beating heart on a chip^[21,22] and the MPCC on a chip^[20] were adapted in this device which is obtained by the consecutive assembly of three PDMS layers named chambers, valve, and actuation layers.

The chambers layer (i.e., bottom layer, Figure 4A(i)) features two culture chambers to host the hepatic and the cardiac models. In detail, the hepatic chamber is an oval-shaped chamber 3.5 mm wide, 8 mm long, and 0.15 mm high. It has one inlet and one outlet for cell seeding and medium supply. The chamber is isolated from its reservoirs by dead-end channels which will generate PDMS walls of 250 \times 500 μ m width. The heart chamber is composed of two lateral channels for medium replenishment, partially separated by two parallel rows of shield-shaped hanging posts (100 μ m high, 110 μ m long, 60 μ m wide, and 110 μ m center-to-center spaced) from a central channel 300 μ m wide. At the edges of this central channel there are an inlet and an outlet to inject

the cell laden hydrogel. Underneath the posts there is a 50 μ m-height gap that serves to precisely control the provided mechanical stimulation. Moreover, four guides for electrode insertion were designed at the two opposite ends of the central channel hosting the cardiac microtissue, so to obtain an integrated electrical readout system, which is fundamental to collect information about tissue maturation and response to stimuli (e.g., drug administration).^[33] The two chambers are separated by four 1000 \times 500 μ m dead-end channels where PDMS walls (250 \times 500 μ m wide) will be generated to isolate the two compartments. These PDMS walls can be lifted up all at the same time through a superimposed valve layer.

The valve layer (i.e., middle layer, Figure 4A(ii)) contains two on/off valve systems capable to lift up the PDMS walls of the chambers layer and thus operate the device. In particular, the LivHeart platform features a communication and a liver-reservoir valve system. The communication valve system consists of four circular doormat valves, 1 mm in diameter, connected by a channel that ends with a common vacuum access. The liver-reservoir valves system consists of two circular doormat valves, 1 mm in diameter, connected by a channel that allows to simultaneously operate all of them by means of one single connection port. This reservoir valve is located in correspondence of the reservoir PDMS walls at the entrance and at the exit of the liver culture chamber and is useful to ensure a fine control of fluid diffusion and avoid the convection and dilution of solutes during culture chambers communication. The systems of walls/valves allow an independent maturation of hepatic and cardiac microtissues, and once the chambers and valve layers are coupled, the suction effect caused by vacuum deflects upward the walls in the chambers layer, thus enabling the communication between the two compartments. Alignment signs (i.e., crosses) are present around the liver chamber to ensure the correct alignment of the valve layer on the chamber layer.

The actuation layer (i.e., top layer, Figure 4A(iii)) is designed to provide mechanical stimulation to the 3D cardiac tissue. The actuation chamber is a rectangle of 3 \times 9 mm which is provided with 6 rows of circular pillars of 60 μ m diameter and 450 μ m center-to-center spaced, to prevent the structure buckling during stimulation. The rectangular-shaped chamber is connected through a channel to the actuation access port. Thanks to a correct alignment of the valve and chambers layers, the actuation system can correctly operate the central channel of the heart chamber. In detail, at rest, the gap underneath the hanging pillars of the heart chamber is 50 μ m and the cell-laden gel is unstimulated. When a positive pressure is applied to the actuation layer, the actuation chamber deflects downward the underlying layer and the gap underneath the pillars decreases progressively. As the gap decreases, the cell-laden gel is unidirectionally stretched.

The fabrication of the silicon wafer master mold was performed by UV maskless photolithography. Briefly, flood exposure was first adopted to increase adherence of SU8 features to the silicon wafer, and then the pattern of each layer was transferred on SU8 photoresist, previously spin-coated on 4 in silicon wafers. Features height was set as follows: 150 μ m for both the chambers and the valve layers and 50 μ m for the actuation layer. Specifically, to obtain 150 and 50 μ m photoresist thickness, SU8-2100 and SU8-2050 were spin-coated at a spinning velocity of 1900 and 3250 rpm, respectively.

Technical Characterization—Valve Systems Calibration: The valve systems should allow a proper opening/closure for cells seeding and fluid diffusion between the hepatic and the cardiac compartment. It was therefore important to identify the minimum vacuum pressure that could drive a proper PDMS wall displacement. Specifically, a Tygon tube (ID 0.50 and OD 1.5 mm, Saint Gobain PPL Corp.) was filled with dyes and plugged into the valve layers access ports. The chambers layers were filled with PBS (Biowest) and the valve layers were filled with a green-colored dye or red-colored dye for the Valve (Figure 1C(ii)) and the LivHeart (Figure 4B) devices, respectively. The Tygon tubes were then connected to a mercury column with a pressure gauge and were actuated with decreasing pressure values in the range of 0 and -600 mmHg with a step of 50 mmHg. For each pressure value an image was taken under an upright microscope (B120c, AmScope, magnification 4X).

The images were analyzed by ImageJ software. In details, the images were first converted into a 16-bit format, a fixed region of interest (ROI, 333×255 pixels) in correspondence of the PDMS wall was selected and then the mean gray intensity value was calculated from the selected ROI, as parameter related to the PDMS wall displacement. Indeed, as the module of the applied pressure increased, the valve region above the PDMS wall became consecutively brighter since the wall progressively moved upward and a white spot showed up becoming wider when the wall reached the ceiling of the valve chamber. From the collected data, three calibration curves (i.e., two communication and one liver-reservoir valve system) were derived to quantify valves operating pressures for $N = 3$ Valve and $N = 4$ LivHeart devices.

Technical Characterization—Mechanical Actuation and Strain Calibration: To obtain a proper maturation, the cardiac construct needs to be stimulated through a cyclic mechanical stimulation, which was ensured by the actuation layer in the LivHeart device. To correctly operate, the actuation layer is filled with PBS, which is then put in pressure to drive the ceiling of the cardiac culture chamber to move toward the coverslip until the posts reach its contact (500 mmHg positive pressure). The deformation of the heart culture chamber is transferred to the cardiac microtissue housed in the central channel as a uniaxial stretch. In particular, the gap between the hanging posts and the glass coverslip regulates the movement, tailoring, the stretching. To characterize the deformation of the construct in relation to the applied pressure, the displacement of spherical beads embedded in fibrin gel (i.e., 10 mg mL⁻¹ fibrinogen with 2.5 U mL⁻¹ thrombin) was evaluated. First, the fibrin gel with embedded red polystyrene microbeads (10 μm, Sigma-Aldrich) was prepared. In detail, 1 μL of thrombin (100 U mL⁻¹, Tisseel Baxter) was added to 1 μL of a microbeads suspension diluted with 18 μL of PBS, and 2 μL of fibrinogen (100 mg mL⁻¹, Sigma) was added to 8 μL of PBS, so to obtain a thrombin solution of 5 U mL⁻¹ and a fibrinogen solution of 20 mg mL⁻¹. These two solutions in equal amount were mixed and 5 μL of the obtained beads-laden fibrin prepolymer solution was injected into the cardiac culture channel of the LivHeart device. The gel reticulation was performed in a humid environment at 37 °C for 8 min and then the cardiac chamber was filled with PBS to maintain the gel hydrated. Subsequently, the actuation chamber was filled with PBS as previously described.^[21] The device was then connected to the mercury column and images of the cardiac culture channel (10X magnification) subjected to 0 (50 μm between posts and coverslip) and 500 mmHg (0 μm between posts and coverslip) pressures were acquired and analyzed with ImageJ. In particular, for each image the distance between a tailored couple of beads was measured (Figure 4C). Specifically, the transversal strain (ϵ_{yy}) was measured comparing the distance at the two different pressures of a couple of beads approximately aligned in the x-direction and located at opposite sides with respect to the longitudinal axis of the cardiac culture channel, as described in the Equation (2.1). The longitudinal strain (ϵ_{xx}) was indeed measured comparing the distance at the two different pressures of a couple of beads approximately aligned in the y-direction and located at opposite sides with respect to the longitudinal axis of the cardiac culture channel, as described in Equation (2.2)

$$\epsilon_{yy} = \frac{\Delta y(P_{max}) - \Delta y(P_{min})}{\Delta y(P_{min})} \quad (2.1)$$

$$\epsilon_{xx} = \frac{\Delta x(P_{max}) - \Delta x(P_{min})}{\Delta x(P_{min})} \quad (2.2)$$

Where $\Delta y(P_{max})$ and $\Delta y(P_{min})$ were the distance in transverse direction between two beads measured at 0 and 500 mmHg, respectively; $\Delta x(P_{max})$ and $\Delta x(P_{min})$ were the distance in longitudinal direction between two beads measured at 0 and 500 mmHg, respectively. The strain was evaluated in $N = 4$ LH devices.

Numerical and Experimental Diffusion Tests: Numerical diffusion simulations were computed with COMSOL Multiphysics (version 6.0) to study the drug diffusion dynamics from the liver to the heart compartment in the LivHeart device. The diffusion simulation was performed modeling the chambers layer as 2D in the open valve configuration (i.e., with the complete communication channels and

without the PDMS walls interrupting it). The drug diffusion was simulated through the Transport of Diluted Species (TDS) interface, calculating the concentration field of a dilute solute in a solvent. A time dependent study of 48 h with 1 h steps was selected. The TDS interface solves the mass conservation equation (Equation (2.3)) for one or more chemical species. In this interface, the mass flux J_i (mol (m² s⁻¹)) defines the mass flux diffusive flux vector (Equation (2.4)). In detail, c_i is the concentration of the species (mol m⁻³), u is the mass averaged velocity vector (m s⁻¹), R_i is the reaction rate (mol (m³ s⁻¹)), and D_i is the diffusion coefficient (m² s⁻¹)

$$\partial c_i / \partial t + \nabla \cdot J_i + u \cdot \nabla c_i = R_i \quad (2.3)$$

$$J_i = -D_i \nabla c_i \quad (2.4)$$

In the TDS interface, the convection option was deselected. The medium was modeled with PBS, while the chambers boundaries and the pillars in the heart chamber were modeled with PDMS. The drug Terfenadine (molecular weight of 471.7 g mol⁻¹) was modeled with a diffusion coefficient of 6×10^{-6} cm² s⁻¹.^[34] This diffusion coefficient was set in all domains occupied by media, whereas in the pillars it was set to 0. The overall domain (i.e., the chambers layer) was partitioned isolating the liver chamber from the rest and the initial drug concentration (C_0) of 10 μM was set within this partitioned domain. The domain was meshed with physics-controlled mesh (free triangular, minimum element size of 7.37 μm and maximum element size of 1.65 mm) and the default elements distribution was selected. From the simulation, 2D color maps of the variation in drug concentration over time were derived (Figure 5A). Variation in drug concentration over time was evaluated along the length of the device (i.e., mean of concentration values were measured over time along two vertical lines, one located in the liver chamber and one between the pillars of the heart chamber) to evaluate the diffusion dynamics.

From the experimental point of view, to assess the diffusion through the microchannels and valve systems in the platforms, RFP-Rhodamine (Alquera) was adopted. In particular, RFP-Rhodamine was diluted in water to obtain a final concentration of 1 mg mL⁻¹ and used to fill the liver inlet channels, while transparent PBS was placed in the heart inlet channels. In the μChannels platform, the liver inlet was filled with 50 μL RFP-Rhodamine, while heart inlet channel was filled with 50 μL transparent PBS. In the Valve platform, the liver inlet was filled with 50 μL RFP-Rhodamine, while heart inlet channel was filled with 50 μL transparent PBS. Subsequently, the communication valve system was opened to let the dye diffuse. In the LivHeart platform, liver-reservoirs valve system was opened so that the 50 μL RFP-Rhodamine in the liver inlet could fill the chamber, while heart inlet channel was filled with 50 μL transparent PBS. Subsequently, the liver-reservoirs valve system was closed, and the communication valve system was opened to let the dye diffuse. Images were taken through a fluorescence microscope (Olympus IX71) every hour up to 8 h and the diffusive behavior was measured 0.2 mm far from the right and left borders of the liver and heart chambers, respectively, with ImageJ software and graphed by GraphPad Prism software.

Cell Culture and Seeding Procedure: Collagen domains of 500 μm-diameter, 1200 μm center-to-center spacing were generated on a glass coverslip simultaneously to devices assembly so to be hosted in the liver chamber of the devices.^[20] After sterilization, the devices were used for cell seeding. HepG2 (human Caucasian hepatocyte cell line, Sigma) cells were expanded in a T125 flask (Corning Life Science) in hepatic medium consisting of Dulbecco's modified eagle medium high glucose (DMEM, 4.5 g L⁻¹ glucose), 10% v/v fetal bovine serum (Hyclone), 100 U mL⁻¹ penicillin and 100 μg mL⁻¹ streptomycin. HepG2 were harvested by incubating the cells at 37 °C with 0.05% trypsin-EDTA for 5 min and collecting them in a 50 mL falcon tube (Corning Life Science). After centrifugation at 220xg for 5 min, the HepG2 were seeded in the liver chamber, on the patterned microfluidic compartments at a density of 5×10^6 cells mL⁻¹ in seeding medium consisting in hepatic medium

without the FBS, as previously described.^[20] After cell attachment the seeding medium was switched to hepatic medium and incubated for 24 h in a humidified incubator at 37 °C and 5% CO₂. The subsequent day, NIH-3T3 murine embryonic fibroblasts were added to the liver chamber. In details, NIH-3T3 were incubated at 37 °C with 0.05% trypsin-EDTA for 5 min, collected in a 50 mL falcon tube and centrifuged at 220xg for 5 min. Cells were then seeded in the devices at a density of 1×10^6 cells mL⁻¹ in order to complete the MPCC liver model. In particular, for the LivHeart device, the liver-reservoirs valve system was opened to allow cell seeding. Neonatal rat cardiomyocytes (NRCMs) were obtained from 2-days old Sprague Dowley Rats, as previously described^[22] and freshly used in the devices. After 24 h from MPCC formation, NRCMs microtissues were generated. In details, NRCMs were incubated at 37 °C with 0.05% trypsin-EDTA for 5 min, collected in a 50 mL falcon tube and centrifuged at 200xg for 5 min. Cardiomyocytes were then suspended in a 10 mg mL⁻¹ fibrin gel (10 mg mL⁻¹ fibrinogen with 2.5 U mL⁻¹ thrombin) at 100×10^6 cells mL⁻¹ and seeded in the heart compartment of the devices. Cell-laden hydrogel reticulation was performed in a humid environment at 37 °C and 5% CO₂ for 8 min and then the medium channels of the cardiac chambers were filled with complete culture medium consisting of 50% hepatic medium and 50% EGM-2 medium (Lonza) supplemented with 2 mg mL⁻¹ of Aminocaproic acid (ACA). Culture medium in the cardiac compartment was changed every 24 h by gradually decreasing ACA concentration: day 0-1 (2 mg mL⁻¹), day 2 (1.6 mg mL⁻¹), day 3 (1.4 mg mL⁻¹), whereas culture medium consisting of 50% hepatic medium and 50% EGM-2 medium (without ACA) was changed daily in the hepatic chamber. The communication valve system of the Valve and LivHeart devices was kept close for all seeding operations until drug administration and metabolism, whereas the liver-reservoirs valve system of the LivHeart device was opened only during medium change.

Compounds Cytotoxicity Assessment: For the drug toxicity investigation, on day 5 of culture (Figures 3A and 6A), solutions of Terfenadine (Sigma-Aldrich), Fexofenadine (MedChemExpress) or DMSO (Sigma-Aldrich) were injected in the liver compartment of the devices to allow MPCC metabolism. All drug solutions were prepared at 10 μM concentration in Sigma). Terfenadine serum-free culture medium composed by 50% DMEM and 50% EGM with 1% ITS+ supplement (Sigma). Terfenadine (1 mM stock) and Fexofenadine (10 mM stock) were diluted 100X and 1000X, respectively, to achieve 10 μM concentration. 16 h after drug administration (day 5 of culture) in the liver compartment, the communication valve systems of the Valve and LivHeart devices were opened (day 6 of culture) to allow the drug diffusion toward the cardiac compartment whereas free drug diffusion (day 5-7 of culture) was happening in the μChannels device. The time (*t*) needed for the metabolized drug to diffuse into the cardiac compartment was calculated through Fick's law (Equations (2.5) and (2.6)) knowing the molecule size (*r*), the diffusion length (*x*), and the diffusion coefficient (*D*)

$$x = \sqrt{2Dt} \quad (2.5)$$

$$D = kT / 6\pi\eta r \quad (2.6)$$

where *k* is the Boltzmann constant, *T* is the temperature at which the diffusion process happens, and *η* is the culture medium viscosity. 24 h after the beginning of controlled drug diffusion (i.e., communication valve system opening, day 7 of culture), the effects of Terfenadine (TER without liver metabolism), free liver-metabolized Terfenadine (TER + FEX), controlled liver-metabolized Terfenadine (TER → FEX), Fexofenadine (FEX), and vehicle control (DMSO) were assessed for cytotoxicity (e.g., viability and modification in electrical activity). In particular, in the TER condition, Terfenadine is administered in the liver chamber of the platforms where no HepG2 cells are cultured, and it could diffuse toward the heart chambers and exert its effect on NRCMs only after communication valve system aperture. The cardiac stimulation in the LivHeart was interrupted during drug analysis. Each experimental condition was carried out in at least triplicate (e.g., viability images and

electrical signals). Data processing and visualization were performed using the ImageJ and GraphPad Prism software, data were tested for normality and presented and analyzed with mean ± SD.

Viability and Functionality Assessment: Cell morphology was monitored through an inverted microscope (Olympus CKX41) with 4X, 10X, and 20X phase contrast objectives. Bright field images of hepatic islands and cardiac microtissues were taken every other day for up to 1 week of culture. Additionally, the presence of a synchronous beating within the cardiac constructs was recorded. Cell viability was assessed through a Live/Dead assay (Sigma-Aldrich): devices were washed with PBS three times and a solution of calcein (2 μM) and ethidium homodimer-1 (4 μM) in PBS was pipetted into the reservoirs of the culture chambers. After an incubation of 15 min at 37 °C in the dark, three fluorescent images per construct were taken at 4X, 10X, and 20X magnifications by means of a fluorescent microscope (Olympus IX71). Cell viability quantification was performed through ImageJ software. In detail, images were imported, and live and dead images of the same area were merged. Green labeled cells (live cells) and red cell nuclei (dead cells) were counted inside a region of interest (ROI). Mean and standard deviation of cell viabilities were calculated and plotted for each experimental condition in at least *N* = 3 ROI.

Immunofluorescence images (10X magnification) of both hepatocytes' islands and cardiac constructs were taken with a fluorescence microscope (Olympus IX71). In detail, albumin staining was performed on the hepatic islands, whereas troponin I and connexin staining were performed on cardiac microtissues. For the fixation procedure, chambers were washed twice with PBS after the removal of media from the reservoirs and paraformaldehyde (PFA) 4% was incubated within the devices for 30 min at room temperature. After 30 min, PFA was removed, chambers were washed again twice with PBS (at each washing cycle, PBS was left in the devices for 10 min) and then incubated for 1h at room temperature with a solution of 0.1% Tween-20 and 5% Goat serum. The solution was then removed from the reservoirs and primary antibody solution of FITC Goat antihuman albumin (Thermo-Fisher Scientific), IgG2a antimouse troponin I (Thermo-Fisher Scientific) and Rabbit antimouse Connexin 43 (Thermo-Fisher Scientific) antibodies diluted 1:200 in 0.5% goat serum was incubated within the devices overnight at 4 °C. The following day, primary solution was removed from the reservoirs and the devices were washed twice with PBS (at each washing cycle, PBS was left in the devices for 20 min). Secondary antibody solution of 647 Goat Anti-mouse IgG2a (ThermoFisher) and 488 Goat Anti-rabbit IgG antibodies (Thermo-Fisher Scientific), with intermediate nuclear staining solution (DAPI, 30 μM) were diluted 1:200 and 1:100, respectively, in 0.5% goat serum and incubated in the device for 6 h at 4 °C in the dark. Each experimental condition was carried out at least in triplicate. Data processing and visualization were performed using ImageJ and GraphPad Prism software.

The electrical activity of the cardiac microtissues within the LivHeart device was evaluated 24 h after drug diffusion (i.e., 1 day after communication valve system was opened). Stainless-steel microelectrodes were manually inserted in the microelectrodes coaxial guides till the tip reached the end of the cardiac microtissue (Figure 6C(i)). An AgCl ground electrode was placed into one of the four cardiac reservoirs. Measuring electrodes (two for each microtissues, one at each end) and the AgCl were connected to an extracellular amplifier (Ext-02b, Npi Electronic GmbH, Germany) and the signals were filtered (3 Hz high pass, 10 kHz low pass) and simultaneously amplified (10 k Gain). The electrical signals were acquired and recorded with a rate of 2000 samples per second (i.e., 2 kHz) by means of an electronic board (Analog Discovery 2, Digilent, Washington, USA) connected to a personal computer. From the recorded electrical signals, two parameters were evaluated: the interval between two consecutive R peaks (i.e., depolarization peaks), named beating period (BP) interval, and the field potential duration (FPD) which is the interval measured from the depolarization peak to the repolarization peak (Figure 6C(ii)). The two parameters were manually measured within Waveform software and averaged for each condition. From the mean value of the BP intervals, the spontaneous beat frequency value was derived (Equation (2.7))

and the FPD mean values were corrected with the Fridericia correction (Equation (2.8))

$$\text{Frequency [Hz]} = 1/(\text{BP [s]}) \quad (2.7)$$

$$\text{FPDc [s]} = \text{FPD [s]} \cdot \text{BP}^{1/3} \quad (2.8)$$

Mass Spectrometry: Terfenadine and Fexofenadine incubated in the chip with or without hepatocytes were detected by Multiple Reaction Monitoring (MRM) mass spectrometry using a Xevo TQ-S micro triple quadrupole (Waters, Milford, MA). Samples were mixed with 200 μL of methanol: acetonitrile/1:4 and centrifuged for 5 min at 5000xg. Supernatants were recovered and 50 μL were transferred in a glass vial with 150 μL methanol: acetonitrile 1:1. A volume of 2 μL was injected and separated on a C18 Acquity Premier BEH 100 mm \times 2.1 mm id, 1.7 μm (Waters) kept at 40 $^{\circ}\text{C}$, with the following gradient: 0.0 min: 5% B; 0.5 min: 5% B, 0.51 min: 50% B, 4.5 min: 80% B, 4.51 min 99% B = 5 min 99% B, 5.1 min:5% B at 0.5 mL min⁻¹ flow rate. The mobile phase consisted of solvent A (0.1% formic acid in water) and solvent B (0.1% formic acid in acetonitrile). An electrospray interface operating in positive ion mode was employed to obtain MS/MS spectra by acquiring MRM transitions of terfenadine, 472.28 > 436.29, cone voltage 16 V, collision energy 22 eV and fexofenadine, 502.26 > 466.33, cone voltage 18 V, collision energy 26 eV. The capillary voltage was set at 3.5 kV. The source temperature was set to 150 $^{\circ}\text{C}$. The desolvation gas flow was set to 1000, and the desolvation temperature was set to 350 $^{\circ}\text{C}$. Data were acquired by MassLynx 4.2 software and quantified by TargetLynx software.

Ethical Statement: In this Study, animals involved and euthanized in another study unrelated to this research and approved by the Institutional Animal Care and Use Committee of the San Raffaele Scientific Institute (autorizzazione alla soppressione 02.19) were exploited. All the applicable international, national and/or institutional guidelines for the use of these animals were followed.

Supporting Information

Supporting Information is available from the Wiley Online Library or from the author.

Acknowledgements

The authors thank Claudia Caporale for optimizing liver and cardiac cell culture in the platform. They are grateful to Dr. Barbara Bettegazzi for the kind provision of rat cardiac hearts. The device manufacture was partially performed at PoliFAB, the micro- and nanofabrication facility of Politecnico di Milano. This work was partially financed by the Italian Ministry of Health (Ricerca Finalizzata GR-2016-02364990) and by CARIPLO Foundation, Grant No. 2018-0551.

Open access funding provided by Politecnico di Milano within the CRUI-CARE agreement.

Conflict of Interest

The authors declare no conflict of interest. M.R., P.O., and R.V. have ownership interest in BiomimX S r l, a Politecnico di Milano spin-off which is owner of μECG patent and has exclusive license of uBeat technology.

Author Contributions

E.F. and R.V. contributed equally to this work. E.F., R.V., P.O. and M.R. conceived the project. E.F., R.V. and E.M. designed the devices. E.F. and

E.M. produced the devices. E.F., R.V. and E.M. performed and analyzed the readout of the experiments. E.F., R.V., P.O. and M.R. contributed to the interpretation of results. E.T. performed the mass spectrometry assay. E.F. R.V. and E.M. wrote and revised the manuscript from the input of M.R., P.O. and M.M.

Data Availability Statement

The data that support the findings of this study are available from the corresponding author upon reasonable request.

Keywords

cardiac model, cardiotoxicity, drug safety, hepatic model, liver metabolism, multi Organs-on-chip

Received: September 1, 2022

Revised: December 15, 2022

Published online:

- [1] I. V. Hinkson, B. Madej, E. A. Stahlberg, *Front. Pharmacol.* **2020**, *11*, 770.
- [2] D. Sun, W. Gao, H. Hu, S. Zhou, *Acta Pharm. Sin. B* **2022**, *12*, 3049.
- [3] E. M. Tosca, R. Bartolucci, P. Magni, I. Poggesi, *Expert Opin. Drug Discovery* **2021**, *16*, 1365.
- [4] R. J. Weaver, J. P. Valentin, *Toxicol. Sci.* **2019**, *167*, 307.
- [5] J. McKim Jr., *Comb. Chem. High Throughput Screen* **2010**, *13*, 188.
- [6] J. D. Caplin, N. G. Granados, M. R. James, R. Montazami, N. Hashemi, *Adv. Healthcare Mater.* **2015**, *4*, 1426.
- [7] G. S. Ugolini, D. Cruz-Moreira, R. Visone, A. Redaelli, M. Rasponi, *Micromachines* **2016**, *7*, 233.
- [8] E. Ferrari, M. Rasponi, *APL Bioeng.* **2021**, *5*, 031505.
- [9] M. Carlos-Oliveira, F. Lozano-Juan, P. Occhetta, R. Visone, M. Rasponi, *Biophys. Rev.* **2021**, *13*, 717.
- [10] C. Zuppinger, *Front. Cardiovasc. Med.* **2019**, *6*, 87.
- [11] S. H. Lee, J. H. Sung, *Adv. Healthcare Mater.* **2018**, *7*, 1700419.
- [12] T. Shroff, K. Aina, C. Maass, M. Cipriano, J. Lambrecht, F. Tacke, A. Mosig, P. Loskill, *Open Biol.* **2022**, *12*, 2010333.
- [13] N. Picollet-D'hahan, A. Zuchowska, I. Lemeunier, S. Le Gac, *Trends Biotechnol.* **2021**, *39*, 788.
- [14] Y. Zhao, R. K. Kankala, S. Bin Wang, A. Z. Chen, *Molecules* **2019**, *24*, 675.
- [15] M. B. Esch, A. S. T. Smith, J. M. Prot, C. Oleaga, J. J. Hickman, M. L. Shuler, *Adv. Drug Deliv. Rev.* **2014**, *69–70*, 158.
- [16] C. Oleaga, A. Riu, S. Rothenmund, A. Lavado, C. W. McAleer, C. J. Long, K. Persaud, N. S. Narasimhan, M. Tran, J. Roles, C. A. Carmona-Moran, T. Sasserath, D. H. Elbrecht, L. Kumanchik, L. Richard Bridges, C. Martin, M. T. Schnepfer, G. Ekman, M. Jackson, Y. I. Wang, J. J. Hickman, *Biomaterials* **2018**, *182*, 176.
- [17] C. W. McAleer, A. Pointon, C. J. Long, R. L. Brighton, B. D. Wilkin, L. R. Bridges, N. Narasimhan Sriram, K. Fabre, R. McDougall, V. P. Muse, J. T. Mettetal, A. Srivastava, D. Williams, M. T. Schnepfer, J. L. Roles, M. L. Shuler, J. J. Hickman, L. Ewart, *Sci. Rep.* **2019**, *9*, 9619.
- [18] A. Skardal, S. V. Murphy, M. Devarasetty, I. Mead, H. W. Kang, Y. J. Seol, Y. S. Zhang, S. R. Shin, L. Zhao, J. Aleman, A. R. Hall, T. D. Shupe, A. Kleensang, M. R. Dokmeci, S. Jin Lee, J. D. Jackson, J. J. Yoo, T. Hartung, A. Khademhosseini, S. Soker, C. E. Bishop, A. Atala, *Sci. Rep.* **2017**, *7*, 8837.
- [19] F. Yin, Xu Zhang, L. Wang, Y. Wang, Y. Zhu, Z. Li, T. Tao, W. Chen, H. Yu, J. Qin, *Lab Chip* **2020**, *21*, 571.

- [20] E. Ferrari, G. S. Ugolini, C. Piutti, S. Marzorati, M. Rasponi, *Biomed. Mater.* **2021**, *16*, 045032.
- [21] A. Marsano, C. Conficconi, M. Lemme, P. Occhetta, E. Gaudiello, E. Votta, G. Cerino, A. Redaelli, M. Rasponi, *Lab Chip* **2016**, *16*, 599.
- [22] R. Visone, G. S. Ugolini, D. Cruz-Moreira, S. Marzorati, S. Piazza, E. Pesenti, A. Redaelli, M. Moretti, P. Occhetta, M. Rasponi, *Biofabrication* **2021**, *13*, 035026.
- [23] E. Amaterz, A. Bouddouch, A. Tara, A. Taoufyq, Z. Anfar, B. Bakiz, L. Bazzi, A. Benlhachemi, O. Jbara, *Electrocatalysis* **2020**, *11*, 642.
- [24] R. Visone, G. S. Ugolini, V. Vinarsky, M. Penati, A. Redaelli, G. Forte, M. Rasponi, *Adv. Mater. Technol.* **2019**, *4*, 1800319.
- [25] D. Cruz-Moreira, R. Visone, F. Vasques-Nóvoa, A. S. Barros, A. Leite-Moreira, A. Redaelli, M. Moretti, M. Rasponi, *Biotechnol. Bioeng.* **2021**, *118*, 3128.
- [26] Y. Nozaki, Y. Honda, S. Tsujimoto, H. Watanabe, T. Kunimatsu, H. Funabashi, *Toxicol. Appl. Pharmacol.* **2014**, *278*, 72.
- [27] H. Ohtani, E. Hanada, M. Hirota, H. Sato, H. Kotaki, Y. Sawada, H. Uemura, H. Nakaya, T. Iga, *J. Pharm. Pharmacol.* **2010**, *51*, 1059.
- [28] C. Chen, *Drugs R D* **2007**, *8*, 301.
- [29] R. Vaja, M. Rana, *Anaesth. Intensive Care Med.* **2020**, *21*, 517.
- [30] R. Visone, G. S. Ugolini, D. Cruz-Moreira, S. Marzorati, S. Piazza, E. Pesenti, A. Redaelli, M. Moretti, P. Occhetta, M. Rasponi, *Biofabrication* **2021**, *13*, 035026.
- [31] T. Azar, J. Sharp, D. Lawson, *J. Am. Assoc. Lab Anim. Sci.* **2011**, *50*, 175.
- [32] S. P. Wells, H. M. Waddell, C. B. Sim, S. Y. Lim, G. B. Bernasochi, D. Pavlovic, P. Kirchhof, E. R. Porrello, L. M. D. Delbridge, J. R. Bell, *Am. J. Physiol. Cell Physiol.* **2019**, *317*, C1256.
- [33] E. Ferrari, C. Palma, S. Vesentini, P. Occhetta, M. Rasponi, *Biosensors* **2020**, *10*, 110.
- [34] M. P. Di Cagno, F. Clarelli, J. Vabenø, C. Lesley, S. D. Rahman, J. Cauzzo, E. Franceschinis, N. Realdon, P. C. Stein, *Mol. Pharm.* **2018**, *15*, 1488.